International Journal of Engineering

Journal Homepage: www.ije.ir

TECHNICAL NOTE

Lattice Boltzmann Simulation of Nanofluids Natural Convection Heat Transfer in Concentric Annulus

H. R. Ashorynejad * [a], M. Sheikholeslami [b], E. Fattahi [b]

[a] *Department of Mechanical Engineering, University of Guilan, Rasht, Islamic Republic of Iran*
[b] *Department of Mechanical Engineering, Babol University of Technology, Babol, Islamic Republic of Iran*

PAPER INFO

Paper history:
Received 22 Agust 2012
Received in revised form 18 February 2013
Accepted 18 April 2013

Keywords:
Lattice Boltzmann Method
Nanofluid
Curved Boundary
Natural Convection
Concentric Annulus
Heat Transfer

ABSTRACT

This study is applied Lattice Boltzmann Method to investigate the natural convection flow utilizing nanofluids in a concentric annulus. A numerical strategy presents for dealing with curved boundaries of second order accuracy for both velocity and temperature fields. The fluid between the cylinders is a water-based nanofluid containing different types of nanoparticles: copper (Cu), alumina (Al_2O_3), titanium oxide (TiO_2) and silver (Ag). The nanofluid is a two component mixture modeled as a single-phase incompressible fluid with the different thermophysical properties. This investigation compared with other experimental and found to be in excellent agreement. Result shows The type of nanofluid is a key factor for heat transfer enhancement. In this study the highest values of percentage of heat transfer enhancement are obtained when using silver nanoparticle.

doi: *10.5829/idosi.ije.2013.26.08b.11*

1. INTRODUCTION

Natural convective heat transfer in horizontal annuli has attracted much attention in recent years due to its wide applications such as in solar collector-receiver, underground electric transmission cables, vapor condenser for water distillation and food processing. Numerical simulation of natural convection in concentric and eccentric circular cylinders has been studied rigorously in the literatures[1, 2]. Kuhen and Goldsein [3, 4] conducted experimental and theoretical study of natural convection in concentric and eccentric horizontal cylindrical annuli. Their experimental data is commonly used to validate most of the recent numerical studies. Ho and Lin [5] presented headlines for steady laminar two dimensional natural convection in concentric and eccentric horizontal cylindrical annuli with mixed boundary conditions. Glakpe et al. [1] presented numerical solutions for steady laminar two dimensional natural convection in annuli between concentric and vertically eccentric horizontal circular cylinders. Guj and Stella [6] presented numerical and experimental buoyancy driven flow in horizontal annulus. They studied the effect of the horizontal eccentricity and found that the average Nusselt number is nearly independent of the horizontal eccentricity.

Taking into account the rising demands of modern technology, including chemical production, power generation and microelectronics, there is a need to develop new types of fluids that will be more effective in terms of heat exchange performance. The term 'nanofluid' is envisioned to describe a fluid in which nanometer-sized particles are suspended in conventional heat transfer basic fluids [7].Convectional heat transfer fluids, including oil, water, and ethylene glycol mixture are poor heat transfer fluids, while the thermal conductivity of these fluids play important role on the heat transfer coefficient between the heat transfer medium and the heat transfer surface [8]. Numerous models and methods have been proposed by different authors to study convective flows of nanofluids and we mention here the papers by Khan et al. [9], Vajravelu et al. [10], Yacob et al. [11], etc.

The lattice Boltzmann method (LBM) is a powerful numerical technique based on kinetic theory for simulating fluid flows and modeling the physics in fluids [12, 13]. In comparison with the conventional

* Corresponding Author Email: Ashorynejad@phd.guilan.ac.ir (H. R. Ashorynejad)

CFD methods, the advantages of LBM include simple calculation procedure, simple and efficient implementation for parallel computation, easy and robust handling of complex geometries. Various numerical simulations have been performed using different thermal LB models or Boltzmann-based schemes to investigate the natural convection problems [14, 15]. They have been used for simulation of the flow field in wide range of engineering applications such as natural convection [16], porous media [17], multiphase flow [18], nanofluid flow [19], MHD flow [20], and so on. Several numerical studies on the modeling of natural convection heat transfer in nanofluids have been published recently [21-24].

This paper presents Lattice Boltzmann Method for heat and fluid flow of nanofluids in concentric annulus. Different types of nanoparticles as copper (Cu), alumina (Al_2O_3), titanium oxide (TiO_2) and silver (Ag) with water as their base fluid has been considered. Effects of nanoparticle volume fraction, types of nanofluid, Rayleigh numbers and aspect ratios on the flow and heat transfer characteristics have been examined.

2. PROBLEM DEFINITION AND MATHEMATICAL MODEL

2. 1. Problem Statement The physical model used in this work is shown in Figure 1. A two dimensional horizontal annulus with an inner radius R_i and an outer radius R_o is used. Both cylinders rotate, the inner rotates clockwise, while the outer rotates counterclockwise. γ is measured counterclockwise from the upward vertical plane through the center of the outer cylinders. The inner and outer cylinder surfaces are maintained at different uniform temperatures T_h and T_c respectively, where $(T_h > T_c)$ is assumed. In Figure 1, $\lambda = R_o / R_i$ denotes aspect ratio.

2. 2. The Lattice Boltzmann Method The LB model used here is the same as that employed in [14]. The thermal LB model utilizes two distribution functions, f and g, for the flow and temperature fields, respectively. It uses modeling of movement of fluid particles to capture macroscopic fluid quantities such as velocity, pressure, temperature. In this approach, the fluid domain discretized to uniform Cartesian cells. Each cell holds a fixed number of distribution functions, which represent the number of fluid particles moving in these discrete directions. The D2Q9 model was used and values of $w_0 = 4/9$ for $|c_0| = 0$ (for the static particle), $w_{1-4} = 1/9$ for $|c_{1-4}| = 1$ and $w_{5-9} = 1/36$ for $|c_{5-9}| = \sqrt{2}$ are assigned in this model (Figure 2).

The density and distribution functions i.e. the f and g, are calculated by solving the Lattice Boltzmann equation (LBE), which is a special discretization of the kinetic Boltzmann equation. After introducing BGK approximation, the general form of lattice Boltzmann equation with external force is:

For the flow field:

$$f_i(x + c_i \Delta t, t + \Delta t) = f_i(x,t) + \frac{\Delta t}{\tau_v}[f_i^{eq}(x,t) - f_i(x,t)] + \Delta t c_i F_k \tag{1}$$

and for the temperature field:

$$g_i(x + c_i \Delta t, t + \Delta t) = g_i(x,t) + \frac{\Delta t}{\tau_C}[g_i^{eq}(x,t) - g_i(x,t)] \tag{2}$$

where Δt denotes lattice time step, c_i the discrete lattice velocity in direction i, F_k the external force in direction of lattice velocity, and τ_v and τ_C denotes the lattice relaxation time for the flow and temperature fields.

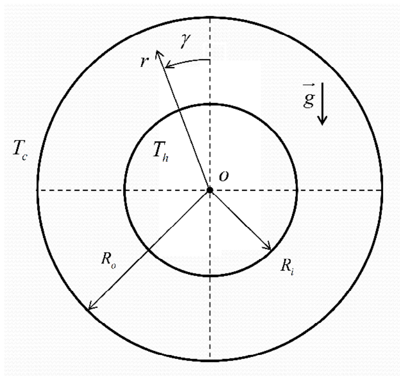

Figure 1. Geometry of the problem

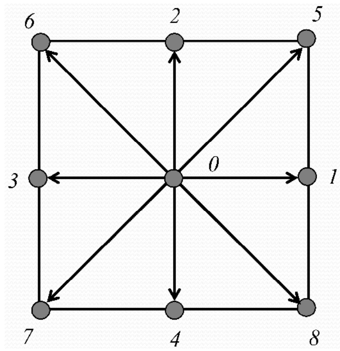

Figure 2. Discrete velocity set of two-dimensional nine-velocity (D2Q9) model.

The kinetic viscosity υ and the thermal diffusivity α, are defined in terms of their respective relaxation times, i.e. $\upsilon = c_s^2(\tau_v - 1/2)$ and $\alpha = c_s^2(\tau_C - 1/2)$, respectively. Note that the limitation $0.5 < \tau$ should be satisfied for both relaxation times to ensure that viscosity and thermal diffusivity are positive. Furthermore, the local equilibrium distribution function determines the type of problem that needs to solve. It also models the equilibrium distribution functions, which are calculated with Equations (3) and (4) for flow and temperature fields respectively.

$$f_i^{eq} = w_i \rho \left[1 + \frac{c_i.u}{c_s^2} + \frac{1}{2}\frac{(c_i.u)^2}{c_s^4} - \frac{1}{2}\frac{u^2}{c_s^2} \right] \quad (3)$$

$$g_i^{eq} = w_i T \left[1 + \frac{c_i.u}{c_s^2} \right] \quad (4)$$

where w_i is a weighting factor and ρ the lattice fluid density.

In order to incorporate buoyancy force in the model, the force term in Equation (1) needs to be calculated in vertical direction (y) as below:

$$F = 3 w_i g_y \beta \theta \quad (5)$$

For natural convection, the Boussinesq approximation is applied and radiation heat transfer is negligible. To ensure that the code works in near incompressible regime, the characteristic velocity of the flow for natural ($V_{natural} \equiv \sqrt{\beta g_y \Delta T H}$) regime must be small compared with the fluid speed of sound. In the present study, the characteristic velocity selected as 0.1 of speed of sound. Finally, macroscopic variables aare calculated with the following formula:

$$\begin{aligned} &\text{Flow density}: \ \rho = \sum_i f_i, \\ &\text{Momentum}: \ \rho \mathrm{u} = \sum_i \mathrm{c}_i f_i, \\ &\text{Temperature}: \ T = \sum_i g_i. \end{aligned} \quad (6)$$

2. 3. Boundary Conditions

2. 3. 1. Curved Boundary Treatment for Velocity

For treating velocity and temperature fields with curved boundaries, the method proposed in [25] has been used. An arbitrary curved wall separating a solid region from fluid is shown in Figure 3. The link between the fluid node x_f and the wall node x_w intersects the physical boundary at x_b. The fraction of the intersected link in the fluid region is $\Delta = |x_f - x_w| / |x_f - x_b|$. To calculate the post-collision distribution function $\tilde{f}_{\bar{\alpha}}(x_b, t)$ based upon the surrounding nodes information, a Chapman–Enskog expansion for the post-collision distribution function on the right-hand side of Equation (1) is conducted as:

$$\tilde{f}_{\bar{\alpha}}(x_b, t) = (1-\chi)\, \tilde{f}_{\alpha}(x_f, t) + \chi\, f_{\alpha}^{*}(x_b, t) + 2 w_{\alpha} \rho \frac{3}{c^2} \mathrm{e}_{\bar{\alpha}}.\mathrm{u}_w \quad (7)$$

where

$$\begin{aligned} & f_{\alpha}^{*}(x_b, t) = w_{\alpha} \rho(x_f, t) \frac{3}{c^2} e_{\alpha}.\left(u_{bf} - u_f\right) + f_{\alpha}^{eq}(x_f, t) \\ & \mathrm{u}_{bf} = \mathrm{u}_{ff} = u(x_{ff}, t), \\ & \chi = \frac{(2\Delta - 1)}{\tau - 2}, \quad if \ \ 0 \le \Delta \le \frac{1}{2} \\ & \mathrm{u}_{bf} = \frac{1}{2\Delta}(2\Delta - 3) u_f + \frac{3}{2\Delta} u_w, \\ & \chi = \frac{(2\Delta - 1)}{\tau - 1/2}, \quad if \ \ \frac{1}{2} \le \Delta \le 1 \end{aligned} \quad (8)$$

In the above, $e_{\bar{\alpha}} \equiv -e_{\alpha}$; u_f is the fluid velocity near the wall; u_w is the velocity of solid wall and u_{bf} is an imaginary velocity for interpolations.

2. 3. 1. Curved Boundary Treatment for Temperature

Following the work of Yan and Zu [25] the non equilibrium parts of temperature distribution function can be defined as :

$$g_{\bar{\alpha}}(\mathbf{x}_b, t) = g_{\bar{\alpha}}^{eq}(\mathbf{x}_b, t) + g_{\bar{\alpha}}^{neq}(\mathbf{x}_b, t) \quad (9)$$

Substituting Equation (9) into Equation (2) leads to :

$$\tilde{g}_{\bar{\alpha}}(\mathbf{x}_b, t+\Delta t) = g_{\bar{\alpha}}^{eq}(\mathbf{x}_b, t) + (1 - \frac{1}{\tau_s}) g_{\bar{\alpha}}^{neq}(\mathbf{x}_b, t) \quad (10)$$

Obviously, both $g_{\bar{\alpha}}^{eq}(\mathbf{x}_b, t)$ and $g_{\bar{\alpha}}^{neq}(\mathbf{x}_b, t)$ are needed to calculate the value of $\tilde{g}_{\bar{\alpha}}(\mathbf{x}_b, t+\Delta t)$. In Equation (10) the equilibrium part is defined as:

$$g_{\bar{\alpha}}^{eq}(\mathbf{x}_b, t) = w_{\bar{\alpha}} T_b^{*} \left(1 + \frac{3}{c^2} \mathbf{e}_{\bar{\alpha}}.\mathbf{u}_b^{*} \right) \quad (11)$$

where T_b^{*} is defined as a function of $T_{b1} = [T_w + (\Delta - 1) T_f] / \Delta$ and $T_{b2} = [2 T_w + (\Delta - 1) T_{ff}] / (1 + \Delta)$

$$\begin{aligned} & T_b^{*} = T_{b1}, \qquad \text{if } \Delta \ge 0.75 \\ & T_b^{*} = T_{b1} + (1 - \Delta) T_{b2}, \quad \text{if } \Delta \le 0.75 \end{aligned} \quad (12)$$

and u_b^{*} is defined as a function of $u_{b1} = [u_w + (\Delta - 1) u_f] / \Delta$

and $u_{b2} = [2u_w + (\Delta - 1)u_{ff}] / (1 + \Delta)$

$$u_b^* = u_{b1}, \qquad \text{if } \Delta \geq 0.75$$
$$u_b^* = u_{b1} + (1 - \Delta)u_{b2}, \qquad \text{if } \Delta \leq 0.75 \tag{13}$$

The non equilibrium part in Equation (14) is defined as:

$$g_\alpha^{neq}(\mathbf{x}_b, t) = \Delta g_\alpha^{neq}(x_f, t) + (1 - \Delta) g_\alpha^{neq}(x_{ff}, t) \tag{14}$$

2. 3. The Lattice Boltzmann Model for Nanofluid

In order to simulate the nanofluid by the lattice Boltzmann method, because of the interparticle potentials and other forces on the nanoparticles, the nanofluid behaves differently from the pure liquid from the mesoscopic point of view and is of higher efficiency in energy transport as well as better stabilization than the common solid-liquid mixture. For pure fluid in absence of nanoparticles in the enclosures, the governed equations are Equations (1)-(14). However for modeling the nanofluid because of changing in the fluid thermal conductivity, density, heat capacitance and thermal expansion, some of the governed equations should change.

The fluid is a water based nanofluid containing different types of nanoparticles: Cu (copper), Al_2O_3 (alumina), Ag (silver) and TiO_2 (titanium oxide).

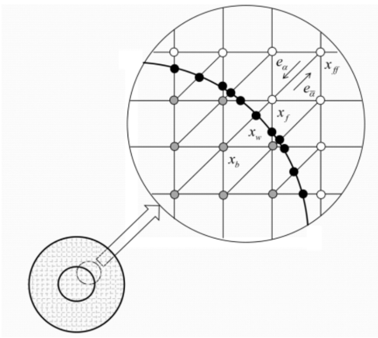

Figure 3. Curved boundary and lattice nodes.

TABLE 1. Thermo physical properties of water and nanoparticles [26].

	ρ (kg/m^3)	C_p (j/kgk)	k (W/mk)	$\beta \times 10^5$ (K^{-1})
Pure water	997.1	4179	0.613	21
Copper (Cu)	8933	385	401	1.67
Silver (Ag)	10 500	235	429	1.89
Alumina (Al_2o_3)	3970	765	40	0.85
Titania (Tio_2)	4250	686.2	8.9538	0.9

The nanofluid is a two component mixture with the following assumptions:

(i) Incompressible;
(ii) No-chemical reaction;
(iii) Negligible viscous dissipation;
(iv) Negligible radiative heat transfer;
(v) Nano-solid-particles and the base fluid are in thermal equilibrium and no slip occurs between them.

The thermo physical properties of the nanofluid are given in Table 1 [26]. The effective density ρ_{nf}, the effective heat capacity $(\rho C_p)_{nf}$ and thermal expansion $(\rho\beta)_{nf}$ of the nanofluid are defined as [27]:

$$\rho_{nf} = \rho_f(1-\phi) + \rho_s\phi \tag{15}$$

$$(\rho C_p)_{nf} = (\rho C_p)_f (1-\phi) + (\rho C_p)_s \phi \tag{16}$$

$$(\rho\beta)_{nf} = (\rho\beta)_f (1-\phi) + (\rho\beta)_s \phi \tag{17}$$

where ϕ is the solid volume fraction of the nanoparticles and subscripts f, nf and s stand for base fluid, nanofluid and solid, respectively.

The viscosity of the nanofluid containing a dilute suspension of small rigid spherical particles is (Brinkman model [28]):

$$\mu_{nf} = \frac{\mu_f}{(1-\phi)^{2.5}} \tag{18}$$

The effective thermal conductivity of the nanofluid can be approximated by the Maxwell–Garnetts (MG) model as [29]:

$$\frac{k_{nf}}{k_f} = \frac{k_s + 2k_f - 2\phi(k_f - k_s)}{k_s + 2k_f + \phi(k_f - k_s)} \tag{19}$$

In order to compare total heat transfer rate, Nusselt number is used. Local Nusselt numbers and the Mean Nusselt number are defined on inner and outer cylinder as:

$$Nu_i = \frac{k_{nf}}{k_f} R_i \ln(R_o / R_i) \left.\frac{\partial T}{\partial r}\right|_{r=R_i}$$
$$Nu_o = \frac{k_{nf}}{k_f} R_o \ln(R_o / R_i) \left.\frac{\partial T}{\partial r}\right|_{r=R_o} \tag{20}$$
$$\overline{Nu} = \frac{k_{nf}}{k_f} \frac{1}{2\pi} \int_0^{2\pi} (Nu)\gamma \, d\gamma$$

And the average Nusselt number is:

$$Nu_{ave} = \frac{\overline{Nu}_i + \overline{Nu}_o}{2} \tag{21}$$

3. RESULTS AND DISCUSSION

In this paper we studied natural convection between two concentric infinite horizontal circular cylinders of inner and outer radius, R_i and R_o, respectively. A radial temperature gradient (ΔT) is applied with subjecting the walls of the inner cylinder to a higher temperature (T_h) than its outer cylinder counterpart (T_c).

Calculations are made for various values of volume fraction of nanoparticle ($\phi = 0, 0.05$ and 0.1), different types of nanoparticles (copper (Cu), alumina (Al_2O_3), titanium oxide (TiO_2) and silver (Ag)), aspect ratios ($\lambda = 2,4,6$ and 8) and Rayleigh numbers ($Ra = 10^4, 5\times 10^4$ and 10^5). It can be seen in Figure 4, for validating the numerical simulation, equivalent thermal conductivity K_{eq} is obtained for a natural convection in concentric horizontal annulus and results have been compared with the study of Kuehn and Goldstein [3]. The average equivalent heat conductivity defined for inner and outer cylinder by:

$$\overline{K_{eq_i}} = -\frac{ln(\lambda)}{\pi(\lambda - 1)}\int_0^{\pi}\frac{\partial T}{\partial r}d\theta$$
$$\overline{K_{eq_o}} = -\frac{\lambda \, . \, ln(\lambda)}{\pi(\lambda - 1)}\int_0^{\pi}\frac{\partial T}{\partial r}d\theta \quad (22)$$

Results represent a good agreement between the present computations and experiments of Kuehn and Goldstein [3]. For further validation, comparisons of isotherms between the present work and experimental studies of Kuehn and Goldstein [3] and Laboni and Guj [30] at the different Rayleigh numbers are shown in Figure 5 (a,b). Furthermore, another validation test was carried for natural convection in an enclosure filled with Cu–water for different Grashof numbers with the results of Khanafer et al. [31] in Figure 6. It is clear that present results are in good agreement with other published data. At last, for final validation this result was compared with study of Abu-Nada [32] which investigated effect of CuO-water nanofluid on natural convection in horizontal annuli by different models of nanofluid. By considering this matter that in this paper M.G. & Brinkman model was used , the results of this paper only were compared by the some part of Abu-Nada results that has used the same model. He introduced normalized Nusselt number as the ratio of Nusselt number at any volume fraction of nanoparticles to that of pure water by following formula:

$$\overset{*}{Nu}_{ave} = \frac{Nu(\varphi)}{Nu(\varphi = 0)} \quad (23)$$

Figure 7 presents the comparison of normalized Nusselt number between this study and Abu-Nada work. It is clear that present results are in good agreement with other published data.

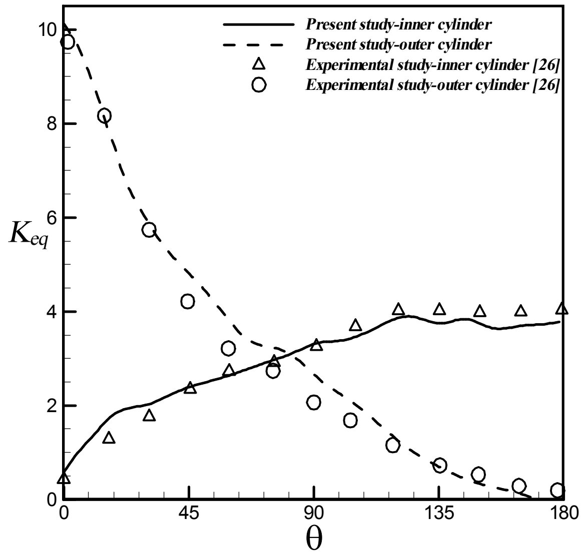

Figure 4. Comparison of equivalent thermal conductivity on inner and outer cylinder with experimental data of Kuehn and Goldstein [3] for viscous flow $(\phi = 0)$, $\lambda = 2.36$, $Ra = 5\times 10^5$

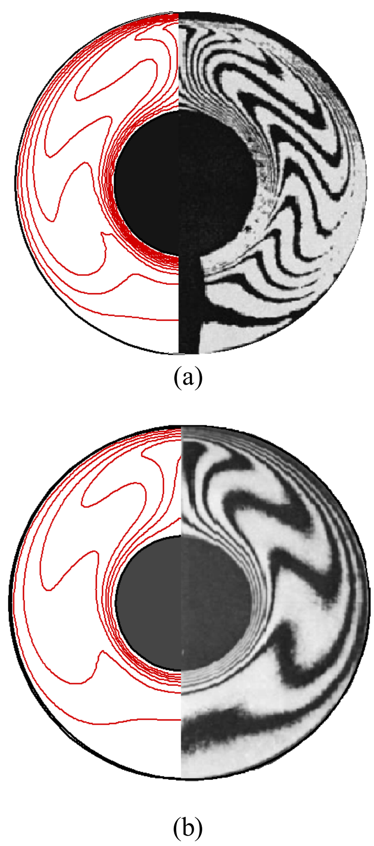

Figure 5. Comparison of present work isotherms with (a) experimental study of Laboni and Guj [30] for $Ra = 0.9 \times 10^5$ and;(b) experimental study of Kuehn and Goldstein [3] for $Ra = 0.9\times 10^5$ and $Pr = 0.71$

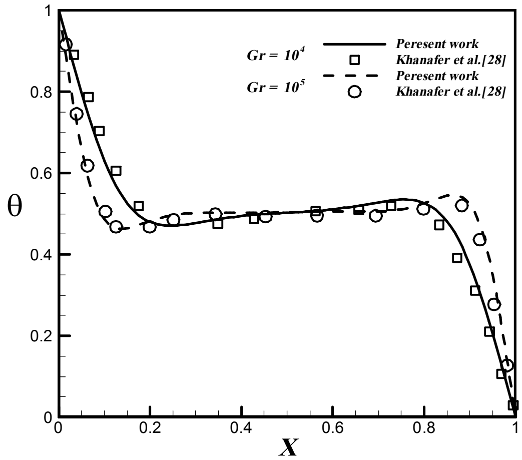

Figure 6. Comparison of the temperature on axial midline between the present results and numerical results by Khanafer et al. [31] $\phi = 0.1$ and $Pr = 6.8(Cu - Water)$.

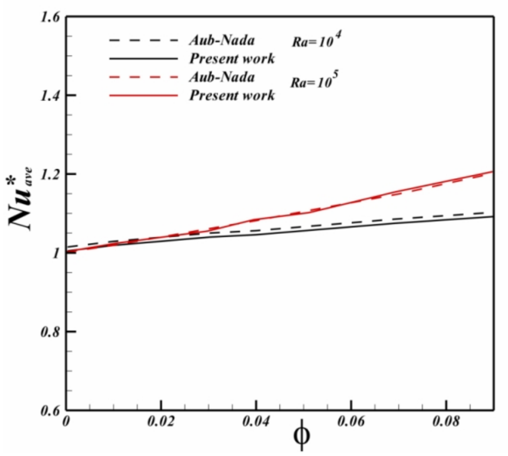

Figure 7. Comparison of normalized Nusselt number between the present results and numerical results Abu-Nada [32] when $L/D = 0.8$ and $Pr = 6.8$

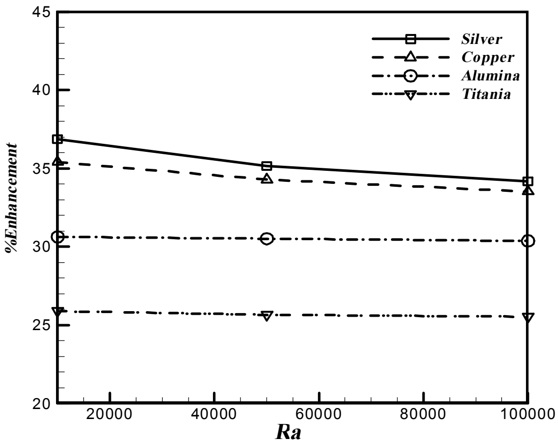

Figure 8. Ratio of enhancement of heat transfer due to addition of nanoparticles for different types of nanofluids when $\lambda = 2$ and $Pr = 6.8$.

The type of nanofluid is a key factor for heat transfer enhancement. So, at first a comparison among different types of nanoparticles is done to select which of them leads to highest cooling performance for this problem.

To estimate the ratio of enhancement of heat transfer between the case of $\phi = 0.1$ and the pure fluid (base fluid) case, the enhancement is defined as:

$$E = \frac{Nu(\phi = 0.1) - Nu(basefluid)}{Nu(basefluid)} \times 100 \quad (23)$$

Figure 8 shows that the ratio of enhancement of heat transfer due to addition of nanoparticles for different types of nanofluids when $\lambda = 2$ and $Pr = 6.8$. For the whole range of Rayleigh number, the figure illustrates that maximum amount of the percentage of heat transfer enhancement is obtained when silver is used as nanoparticle, while minimum amount of it is obtained by selecting titanium oxide.

Also, it can be found that the effect of nanoparticles is more pronounced at low Rayleigh number than at high Rayleigh number because of greater amount of rate of enhancement for low Rayleigh number and increasing Rayleigh number leads to decrease in ratio of enhancement of heat transfer. This observation can be explained by noting that at low Rayleigh number the heat transfer is dominant by conduction. Therefore, the addition of high thermal conductivity nanoparticles will increase the conduction and therefore make the enhancement more effective.

All above mentions indicate that choosing silver leads to highest cooling performance for this problem. Thus in continue effects of various values of volume fraction of nanoparticle, Rayleigh number and aspect ratios angles for Ag-Water case are investigated.

Figure 9 shows that streamline (black) and isotherm (red) for (a) $Ra = 10^4$, (b) $Ra = 5 \times 10^4$ and(c) $Ra = 10^5$ when $\phi = 0.1$,$\lambda = 2$ and Ag-Water case .The effects of Ra and ϕ on (a) $|\psi_{max}|$ and (b) Nusselt number for Cu-Water case when ,$\lambda = 2$ are shown in Figure 10. The velocity components of nanofluid increase as a result of an increase in the energy transport in the fluid with the increasing of volume fraction. Thus, the absolute values of stream functions indicate that the strength of flow increases with increasing of volume fraction of nanofluid (Figure 10 (a)). The sensitivity of thermal boundary layer thickness to volume fraction of nanoparticles is related to the increased thermal conductivity of the nanofluid. In fact, higher values of thermal conductivity are accompanied by higher values of thermal diffusivity. The high value of thermal diffusivity causes a drop in the temperature gradients and accordingly increases the boundary thickness. This increase in thermal boundary layer thickness reduces the Nusselt number, however, according to Equation (20), the Nusselt number is a multiplication of temperature gradient and the thermal conductivity ratio (conductivity of the nanofluid to the conductivity of the base fluid). Since the reduction in temperature gradient due to the presence of nanoparticles is much smaller than thermal conductivity ratio therefore an enhancement in Nusselt is taken place by increasing the volume fraction of nanoparticles (Figure 10(b)).

Figure 11 displays that the streamline (black) and isotherm (red) for (a) $\lambda = 2$,(b) $\lambda = 4$ and (c) $\lambda = 8$ when $\phi = 0.1$, $Ra = 10^4$ and Ag-Water case. Effect of λ on (a)$|\psi_{max}|$ for Ag-Water case when $\phi = 0.1$ are shown in Figure 12. It can be seen that as λ increases, distance between cold wall and hot wall increases that leads to smaller heat transfer rates (Figure 11). Figure 12 shows that by increasing λ, $|\psi_{max}|$ decreases. These changes is more prononced for greater values of Rayleigh number.

Figure 13 shows that the effects of λ and Ra on ratio of enhancement of heat transfer due to addition of nanoparticles for Ag-Water case. It can be found that ratio of enhancement of heat transfer has different behavior for various values of Rayleigh number. As shown in Figure 12 for $Ra = 10^4$ the enhancement in heat transfer decreases with increasing aspect ratio.
When $Ra = 5 \times 10^4$ by increasing aspect ratio from 2 to 8, at first percentage of heat transfer enhancement decreases and then it increases. Also, for $Ra = 10^5$, it can be seen that percentage of heat transfer enhancement profile has one maximum points and one minimum point.

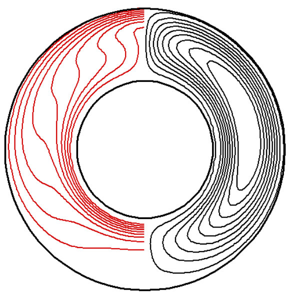

(a)

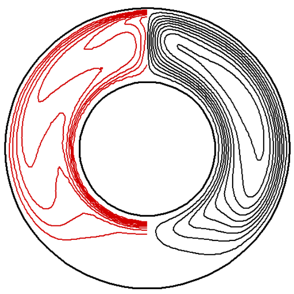

(b)

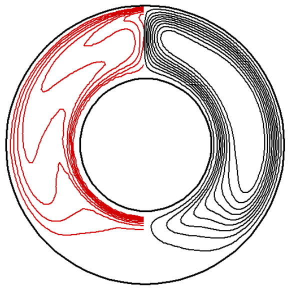

(c)

Figure 9. Streamline (black) and isotherm (red) for (a) $Ra = 10^4$,(b) $Ra = 5 \times 10^4$ and (c) $Ra = 10^5$ when $\phi = 0.1$,$\lambda = 2$ and Ag-Water case

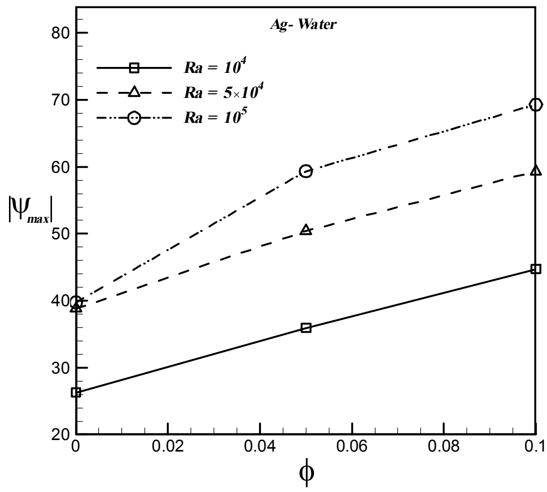

(a)

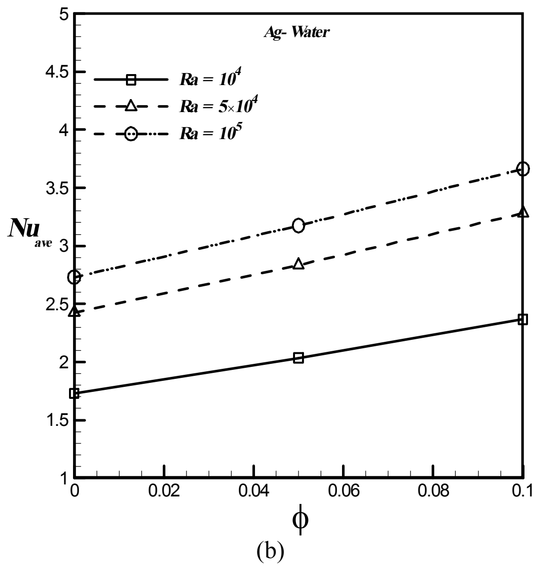

(b)

Figure 10. Effects of Ra and ϕ on (a)$|\psi_{max}|$and (b) Nusselt number for Cu-Water case when ,$\lambda = 2$.

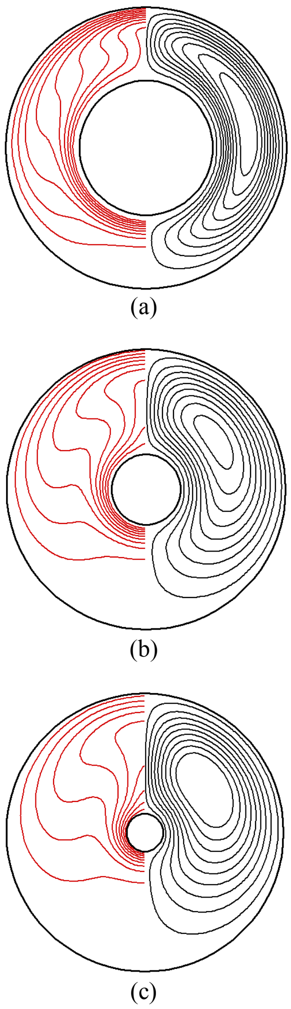

Figure 11. Streamline (black) and isotherm (red) for (a) $\lambda = 2$,(b) $\lambda = 4$ and (c) $\lambda = 8$ when $\phi = 0.1$, $Ra = 10^4$ and Ag-Water case.

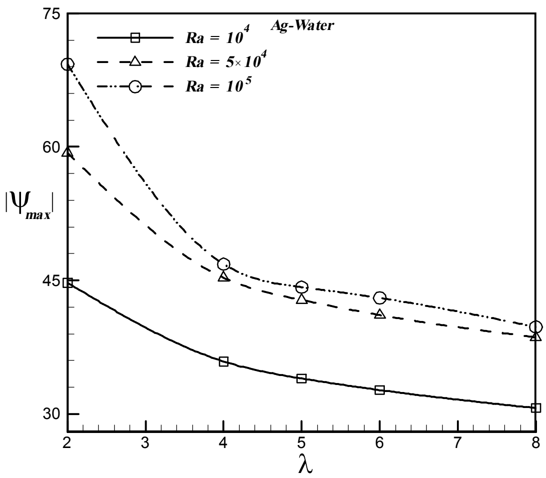

Figure 12. Effect of λ on (a) $|\psi_{max}|$ for Ag-Water case when $\phi = 0.1$.

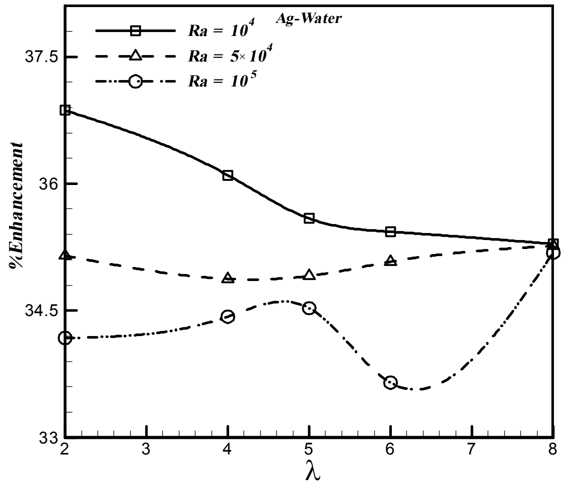

Figure 13. Effects of λ and Ra on ratio of enhancement of heat transfer due to addition of nanoparticles for Ag-Water case.

4. CONCLUSION

In the present study, LBM scheme is applied to investigate natural convection in a concentric annulus using nanofluids. Effects of nanoparticle volume fraction, types of nanofluid, Rayleigh numbers and aspect ratios on the flow and heat transfer characteristics have been examined. Result shows that Lattice Boltzmann method based on double-population is a powerful approach for simulating natural convection in the geometry that include curved boundaries. This method can simulate the velocity and temperature fields with second order accuracy. The type of nanofluid is a key factor for heat transfer enhancement. The highest values of percentage of heat transfer enhancement are obtained when using silver nanoparticle. Also results indicate that Nusselt number is an increasing function of each of nanoparticle volume fraction and Rayleigh numbers and the effect of nanoparticles is more pronounced at low Rayleigh numbers than at high Rayleigh numbers.

5. REFERENCES

1. Glakpe, E., Watkins Jr, C. and Cannon, J., "Constant heat flux solutions for natural convection between concentric and eccentric horizontal cylinders", ***Numerical Heat Transfer, Part A: Applications***, Vol. 10, No. 3, (1986), 279-295.
2. Lee, T., Hu, G. and Shu, C., "Application of gdq method for the study of natural convection in horizontal eccentric annuli", ***Numerical Heat Transfer: Part A: Applications***, Vol. 41, No. 8, (2002), 803-815.
3. Kuehn, T. and Goldstein, R., "An experimental and theoretical study of natural convection in the annulus between horizontal concentric cylinders", ***Journal of Fluid Mechanics***, Vol. 74, No. 4, (1976), 695-719.

4. Kuehn, T. and Goldstein, R., "A parametric study of prandtl number and diameter ratio effects on natural convection heat transfer in horizontal cylindrical annuli", ***Journal of Heat Transfer***, Vol. 102, (1980), 768.

5. Ho, C., Lin, Y. and Chen, T., "A numerical study of natural convection in concentric and eccentric horizontal cylindrical annuli with mixed boundary conditions", ***International Journal of Heat and Fluid Flow***, Vol. 10, No. 1, (1989), 40-47.

6. Guj, G. and Stella, F., "Natural convection in horizontal eccentric annuli: Numerical study", ***Numerical Heat Transfer, Part A: Applications***, Vol. 27, No. 1, (1995), 89-105.

7. Kakac, S. and Pramuanjaroenkij, A., "Review of convective heat transfer enhancement with nanofluids", ***International Journal of Heat and Mass Transfer***, Vol. 52, No. 13, (2009), 3187-3196.

8. Muthtamilselvan, M., Kandaswamy, P. and Lee, J., "Heat transfer enhancement of copper-water nanofluids in a lid-driven enclosure", ***Communications in Nonlinear Science and Numerical Simulation***, Vol. 15, No. 6, (2010), 1501-1510.

9. Khan, W. and Pop, I., "Boundary-layer flow of a nanofluid past a stretching sheet", ***International Journal of Heat and Mass Transfer***, Vol. 53, No. 11, (2010), 2477-2483.

10. Vajravelu, K., Prasad, K., Lee, J., Lee, C., Pop, I., and Van Gorder, R. A., "Convective heat transfer in the flow of viscous Ag–water and Cu–water nanofluids over a stretching surface", ***International Journal of Thermal Sciences***, Vol. 50, No. 5, (2011), 843-851.

11. Yacob, N. A., Ishak, A., Pop, I. and Vajravelu, K., "Boundary layer flow past a stretching/shrinking surface beneath an external uniform shear flow with a convective surface boundary condition in a nanofluid", ***Nanoscale Research Letters***, Vol. 6, No. 1, (2011), 1-7.

12. Yu, D., Mei, R., Luo, L. S. and Shyy, W., "Viscous flow computations with the method of lattice boltzmann equation", ***Progress in Aerospace Sciences***, Vol. 39, No. 5, (2003), 329-367.

13. Succi, S., "The lattice boltzmann equation for fluid dynamics and beyond, clarendon", Oxford, (2001).

14. Kao, P. H. and Yang, R. J., "Simulating oscillatory flows in rayleigh–benard convection using the lattice boltzmann method", ***International Journal of Heat and Mass Transfer***, Vol. 50, No. 17, (2007), 3315-3328.

15. Amaya-Ventura, G. and Rodriguez-Romo, S., "LBM for cyclic voltammetry of electrochemically mediated enzyme reactions and rayleigh-benard convection in electrochemical reactors", ***Heat and Mass Transfer***, Vol. 48, No. 2, (2012), 373-390.

16. Delavar, M. A., Farhadi, M. and Sedighi, K., "Effect of the heater location on heat transfer and entropy generation in the cavity using the lattice boltzmann method", ***Heat Transfer Research***, Vol. 40, No. 6, (2009), 521-536.

17. Hasanpour, A., Farhadi, M., Sedighi, K. and Ashorynejad, H., "Numerical study of prandtl effect on mhd flow at a lid-driven porous cavity", ***International Journal for Numerical Methods in Fluids***, Vol. 70, No. 7, (2012), 886-898.

18. Huang, H., Li, Z., Liu, S. and Lu, X. y., "Shan and chen type multiphase lattice boltzmann study of viscous coupling effects for two-phase flow in porous media", ***International Journal for Numerical Methods in Fluids***, Vol. 61, No. 3, (2009), 341-354.

19. Jafari, M., Farhadi, M., Sedighi, K. and Fattahi, E., "Effect of wavy wall on convection heat transfer of water-Al_2O_3 nanofluid in a lid-driven cavity using lattice boltzmann method", ***International Journal of Engineering-Transactions A: Basics***, Vol. 25, No. 2, (2012), 165.

20. Ashorynejad, H. R., Mohamad, A. A. and Sheikholeslami, M., "Magnetic field effects on natural convection flow of a nanofluid in a horizontal cylindrical annulus using lattice boltzmann method", ***International Journal of Thermal Sciences***, (2012).

21. Ashorynejad, H., Sheikholeslami, M., Pop, I. and Ganji, D., "Nanofluid flow and heat transfer due to a stretching cylinder in the presence of magnetic field", ***Heat and Mass Transfer***, (2013), 1-10.

22. Sheikholeslami, M., Gorji-Bandpay, M. and Ganji, D., "Magnetic field effects on natural convection around a horizontal circular cylinder inside a square enclosure filled with nanofluid", ***International Communications in Heat and Mass Transfer***, (2012).

23. Nemati, H., Farhadi, M., Sedighi, K., Ashorynejad, H. and Fattahi, E., "Magnetic field effects on natural convection flow of nanofluid in a rectangular cavity using the lattice boltzmann model", ***Scientia Iranica***, Vol. 19, No. 2, (2012), 303-310.

24. Domairry, D., Sheikholeslami, M., Ashorynejad, H. R., Gorla, R. S. R. and Khani, M., "Natural convection flow of a non-newtonian nanofluid between two vertical flat plates", ***Proceedings of the Institution of Mechanical Engineers, Part N: Journal of Nanoengineering and Nanosystems***, Vol. 225, No. 3, (2011), 115-122.

25. Choi, S. K. and Lin, C. L., "A simple finite-volume formulation of the lattice boltzmann method for laminar and turbulent flows", ***Numerical Heat Transfer, Part B: Fundamentals***, Vol. 58, No. 4, (2010), 242-261.

26. Oztop, H. F. and Abu-Nada, E., "Numerical study of natural convection in partially heated rectangular enclosures filled with nanofluids", ***International Journal of Heat and Fluid Flow***, Vol. 29, No. 5, (2008), 1326-1336.

27. Xuan, Y. and Roetzel, W., "Conceptions for heat transfer correlation of nanofluids", ***International Journal of Heat and Mass Transfer***, Vol. 43, No. 19, (2000), 3701-3707.

28. Wang, X. Q. and Mujumdar, A. S., "Heat transfer characteristics of nanofluids: A review", ***International Journal of Thermal Sciences***, Vol. 46, No. 1, (2007), 1-19.

29. Abu-Nada, E., Masoud, Z. and Hijazi, A., "Natural convection heat transfer enhancement in horizontal concentric annuli using nanofluids", ***International Communications in Heat and Mass Transfer***, Vol. 35, No. 5, (2008), 657-665.

30. Labonia, G. and Guj, G., "Natural convection in a horizontal concentric cylindrical annulus: Oscillatory flow and transition to chaos", ***Journal of Fluid Mechanics***, Vol. 375, (1998), 179-202.

31. Khanafer, K., Vafai, K. and Lightstone, M., "Buoyancy-driven heat transfer enhancement in a two-dimensional enclosure utilizing nanofluids", ***International Journal of Heat and Mass Transfer***, Vol. 46, No. 19, (2003), 3639-3653.

32. Abu-Nada, E., "Effects of variable viscosity and thermal conductivity of CuO-water nanofluid on heat transfer enhancement in natural convection: Mathematical model and simulation", ***Journal of Heat Transfer***, Vol. 132, No. 5, (2010).

Lattice Boltzmann Simulation of Nanofluids Natural Convection Heat Transfer in Concentric Annulus

TECHNICAL NOTE

H. R. Ashorynejad[a], M. Sheikholeslami[b], E. Fattahi[b]

[a] *Department of Mechanical Engineering, University of Guilan, Rasht, Islamic Republic of Iran*
[b] *Department of Mechanical Engineering, Babol University of Technology, Babol, Islamic Republic of Iran*

PAPER INFO

Paper history:
Received 22 Agust 2012
Received in revised form 18 February 2013
Accepted 18 April 2013

Keywords:
Lattice Boltzmann Method
Nanofluid
Curved Boundary
Natural Convection
Concentric Annulus
Heat Transfer

چکیده

این مطالعه روش شبکه بولتزمن را برای بررسی جریان جابه‌جایی طبیعی درون سیلندر حلقوی هم‌مرکز با استفاده از نانوسیال به کار گرفته است. در محاسبات دما و سرعت برای مرزهای منحنی شکل از دقت مرتبه دوم استفاده شده است. سیال موجود بین سیلندرها متشکل از آب به همراه نانوذرات جامد مختلف از جنس مس (Cu) ، اکسید آلومینیم (Al_2O_3)، اکسید تیتانیم (TiO_2) و نقره (Ag) می باشد. نانو سیال در این جا یک مخلوط دو جزئی تک فاز تراکم‌ناپذیر با خواص ترموفیزیکی متفاوت است. نتایج این مدل با داده های آزمایشگاهی مقایسه، و تطابق بسیار خوبی بین آنها مشاهده شد. نتایج نشان می‌دهد که نوع نانوسیال عامل کلیدی در افزایش انتقال حرارت است.در این مطالعه بیشترین درصد افزایش انتقال حرارت با به کارگیری نانوذرات نقره به دست آمد.

doi: *10.5829/idosi.ije.2013.26.08b.11*